BLE-based Collaborative Indoor Localization with Adaptive Multi-lateration and Mobile Encountering

Jun-Wei Qiu, Chien-Pu Lin, and Yu-Chee Tseng
Dept. of Computer Science, National Chiao-Tung University, Hsin-Chu City 30010, Taiwan
Email: {chiucw, cplin, yctseng}@cs.nctu.edu.tw

***Abstract*— The demands on indoor localization services have grown explosively due to increasing popularity of mobile devices. Though various techniques based on wireless signals have been proposed, the new *Bluetooth 4.0* and *4.1* technologies introduce both opportunities and challenges for localization. Like all wireless signals, the fluctuations caused by hardware conditions and environmental dynamics may deteriorate the accuracy of localization. Therefore, we propose to use *adaptive ranging*, which utilizes inter-beacon measurements to "*sense*" the transient device and environmental conditions, and adjust the parameters of signal propagation model. In this research, we apply this concept to *multi-lateration* and *mobile encountering* for localization using Bluetooth advertisements. We also validate that with the proposed adaptive ranging techniques, the impacts of signal fluctuations caused by hardware and environmental conditions can be greatly decreased. Furthermore, we combine the adaptive multi-lateration, encountering mechanism and pedestrian dead-reckoning with a *particle filter* (PF) framework to generate our localization results. Finally, two sets of experiments are performed in a department building. The overall improvement in accuracy is approximately 19.99% using our adaptive localization when comparing to the conventional non-adaptive methods.**

Keywords: adaptive ranging, Bluetooth 4.1, indoor localization, mobile encountering, particle filter

I. Introduction

The rapid growths of wireless communications and mobile devices have led to an exploding development of *location-based services* (LBS). One of the fundamental technologies in LBS is location tracking. Currently, GPS has been widely used in outdoor environments, but it becomes unavailable in indoor environments. Thus, many alternative indoor localization techniques have been studied and proposed. Some works rely on auxiliary radio-frequency (RF) signals [1, 2]. Such approaches are quite sensitive to signal dynamics. With the newly released *Bluetooth low energy* (BLE) technology in the Bluetooth 4.0 and 4.1 specifications, it is easy to deploy BLE-based beacons as localization infrastructure with low power consumption and cost. However, similar to other wireless systems, Bluetooth also suffers from signal fluctuations caused by environmental dynamics. Hence, pure BLE ranging is still incapable of achieving accurate localization alone. To deal with this problem, we propose to use the *adaptive ranging* technique, which can measure transient environmental conditions using inter-beacon measurements, and adjust the distance estimation models between two devices and thus the localization results.

In this research, we utilize the proposed adaptive ranging technique to estimate two types of distances: *a*) distances between mobile devices and beacons (*D2B* distances) and *b*) distances between mobile devices (*D2D* distances). With the D2B measurements, we can apply *multi-lateration* to infer locations when there are sufficient BLE infrastructures in the environment. On the other hand, if there is no infrastructure coverage, D2D measurements allow us to detect *mobile encountering* among devices and further calibrate their locations through information exchanges also via BLE advertisements. To realise our concept, we implement a localization system using particle filter to fuse the inertial data, adaptive multi-lateration and encountering data together based on the Bluetooth 4.0 and 4.1 protocols. Finally, two experiments are performed to validate our claims.

The rest of this paper is organized as follows. Section II discusses some related works. Section III explains the proposed adaptive ranging technique. Section IV introduces our localization models based on the adaptive concepts. Section V shows our simulation and experiment results. Finally, Section VI concludes this research.

II. Related Work

Due to the unavailability of GPS in indoor environments, many indoor localization systems based on radio-frequency (RF) signals have been proposed. Fingerprinting [1] and lateration/angulation techniques [2, 3] are two of the major RF-based approaches. Bluetooth 4.0 and 4.1 are low-cost, energy-saving technologies currently supported by most commodity devices. Several works have used BLE protocols for localization [4, 5]. In [6], a robot uses BLE infrastructure and locate objects marked with Bluetooth tags. However, these signals are often interfered by environmental dynamics. Some works propose to use extra infrastructural devices to calibrate the signal models [7, 8], or apply sensor-assisted schemes to calibrate the current radio map [9]. Also, reference [10] proposes to use inter-AP measurements to select appropriate WiFi radio maps and proper signal propagation models.

On the other hand, the pedestrian dead-reckoning (PDR) techniques [11, 12] require no auxiliary signal, but they can only obtain relative locations and suffer from accumulative errors. Recently, many systems are designed based on the fusion of inertial and RF observations using particle filter (PF) [13] techniques. In addition to fuse individual devices' own observations, collaborative solutions allow devices to share their observations to improve localization accuracy [14, 15].

978-1-4673-9814-5/16/$31.00 ©2016 IEEE

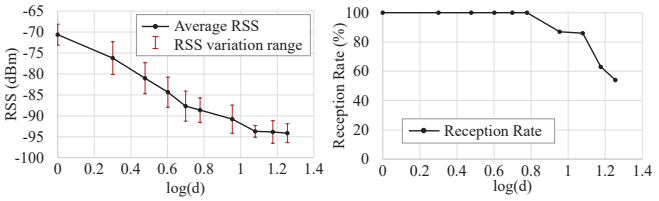

(a) RSS-distances relation. (b) Reception rate.

Fig. 1. BLE signal observations at different distances.

Among all existing works, there is still no research that combines adaptive mechanism with collaborative localization based on a single communication protocol between clients and infrastructure. The purpose of our work is to integrate the advantages of existing collaborative techniques and adaptive ranging concepts together with a particle filter using Bluetooth BLE advertisements for localization.

III. Adaptive Ranging

A. Signal Propagation Models

Ranging by received signal strength (RSS) is a basic operation in RF-based localizations. The log-distance path loss model is commonly used to model the RSS-distance relations, which is formulated as $P = P_0 - 10\gamma \cdot \log(d/d_0)$, where P and d are the RSS in dBm and the physical distance in meters. The constant P_0 is the reference RSS at d_0, and γ is the path-loss exponent. By rearranging the formula as $P = (P_0 + 10\gamma \log d_0) - 10\gamma \log d$, one can conclude that there is a linear relation between the RSS P and $\log d$. To visualize this relation, we collected 100 RSS samples at different distances of 1-6 m, 9 m, 12 m, 15 m and 18 m. The RSS and reception rate at each distance are shown in Fig. 1(a) and Fig. 1(b), respectively. The drop in reception rate at long distances and the minimum RSS a device can report may cause the measurements drift away from expectation. In this research, we apply the propagation models on two ranging applications: *a*) device-to-beacon lateration (D2B distances), and *b*) mobile encountering (D2D distances).

To conquer the signal dynamics caused by environment and device conditions, we use *adaptive ranging* to adjust the parameters of propagation model using inter-beacon measurements in our system. We explain the concepts below: Let X be the ranging device and $b_i, i \in [1, m]$ be a set of beacons, which can transmit and receive BLE messages. Also, let P_{ji} be the average RSS of b_i's advertisements detected by b_j, and d_{ij} be the physical distance between b_i and b_j. Then, we use inter-beacon measurements to *sense* the transient conditions and estimate the parameters of signal propagation model, and therefore, to estimate distance d_{Xi} between X and b_i. According to previous derivation, the obtained P_{ji} and $\log d_{ji}$ should be a sample on the relation $\log d_{ji}{=}\alpha_i P_{ji}{+}\beta_i$. Hence, for each beacon b_i with at least two receivers, linear regression can be applied to derive (α_i, β_i).

A scenario is shown in Fig. 2(a). Assume that $b_j, b_k, b_\ell, ...$ have just received an advertisement from b_i. For each measurement made by b_j on b_i's advertisement, b_j records a sample

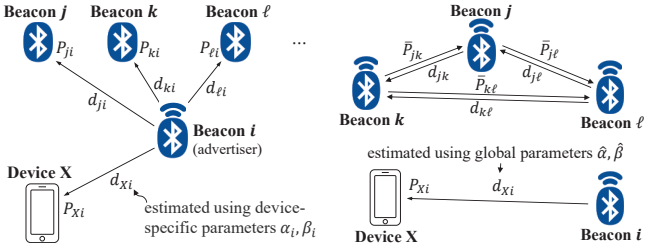

(a) Device-specific parameters. (b) Global parameters.

Fig. 2. Two types of regression parameters for adaptive ranging.

of $(\log d_{ji}, P_{ji})$. After collecting all samples from the beacons that can detect b_i within a pre-defined time period, we can represent the linear relation as $A \times B = C$, where

$$A = \begin{bmatrix} P_{ji} & 1 \\ P_{ki} & 1 \\ P_{\ell i} & 1 \\ \vdots & \vdots \end{bmatrix}, B = \begin{bmatrix} \alpha_i \\ \beta_i \end{bmatrix}, C = \begin{bmatrix} \log d_{ji} \\ \log d_{ki} \\ \log d_{\ell i} \\ \vdots \end{bmatrix}. \quad (1)$$

Applying the least-square analysis $B = (A^T A)^{-1} A^T C$, the device-specific parameters (α_i, β_i) for beacon b_i can be derived and applied to any ranging with b_i.

Unfortunately, some beacons may not have enough measurements to derive their device-specific parameters. Fig. 2(b) shows an example, where beacon b_i is isolated, but b_j, b_k, and b_ℓ can report inter-beacon measurements. In such occasions, the system derives a set of global parameters $(\hat{\alpha}, \hat{\beta})$ representing the overall propagation behaviour by regressing the reports of inter-device measurement from all beacons. The global relation can be formulated as $A \times B = C$, where

$$A = \begin{bmatrix} \bar{P}_{jk} & 1 \\ \bar{P}_{j\ell} & 1 \\ \bar{P}_{k\ell} & 1 \\ \vdots & \vdots \end{bmatrix}, B = \begin{bmatrix} \hat{\alpha} \\ \hat{\beta} \end{bmatrix}, C = \begin{bmatrix} \log d_{jk} \\ \log d_{j\ell} \\ \log d_{k\ell} \\ \vdots \end{bmatrix}, \quad (2)$$

and the power terms $\bar{P}$ in A represent the average bi-directional RSS measurements between two beacons. With the global parameters, we can estimate the distance from a receiver X to beacon b_i even if b_i does not have its specific parameters.

B. Validation Results

To validate our claims, we perform several experiments using HTC Nexus 9 tablets with Bluetooth 4.1 capability under three different environmental conditions: C1) daytime with air-conditioning (25 °C, 999 hPa, 44% humidity), C2) daytime without air-conditioning (30 °C, 999 hPa, 68% humidity), and C3) night without air-conditioning (28 °C, 996 hPa, 56% humidity). We discuss our validations below:

1) RSS Correlation between Different Receivers: We believe that environmental conditions cause similar impacts on RSS from different receivers, and our adaptive scheme can capture this effect and adjust the propagation model accordingly. As shown in Fig. 3(a), we install a transmitter and two receivers. Let $d_1{\in}\{2$ m, 5 m, 10 m$\}$ and $d_2{\in}\{2$ m, 5 m, 10 m$\}$ be the distances from the transmitter to receiver 1 and receiver 2, respectively. We take RSS samples on both receivers every 300 s for 4 hours, and observe the correlations of RSS at

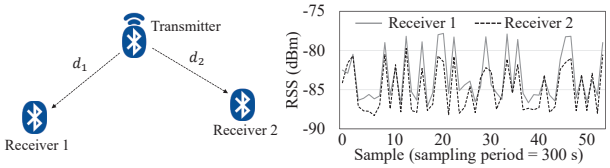

(a) (b)

Fig. 3. Experiment to observe RSS correlations between two receivers: (a) configuration, and (b) RSS on both receivers under C2, where d_1=d_2=5 m.

TABLE I
THE CORRELATION COEFFICIENTS OF RSS UNDER DIFFERENT ENVIRONMENTAL CONDITIONS AND INTER-DEVICE DISTANCES.

	Condition C1			Condition C2			Condition C3		
$d_1 \backslash d_2$	2 m	5 m	10 m	2 m	5 m	10 m	2 m	5 m	10 m
2 m	0.96	0.95	0.79	0.72	0.67	0.67	0.78	0.81	0.84
5 m	0.70	0.59	0.46	0.78	0.91	0.90	0.80	0.73	0.67
10 m	0.73	0.41	0.57	0.65	0.49	0.57	0.62	0.72	0.54

all d_1, d_2 distance configurations under three environmental conditions. Fig. 3(b) shows the RSS values on two receivers where (d_1, d_2)= (5 m, 5 m) under condition C2. The similarity in RSS dynamics can be observed. To further quantify our observations, we show the correlation coefficients of RSS from the two receivers in Table I. The results exhibit high positive correlations in all cases. It implies that our adaptive scheme can capture these dynamics and achieve higher accuracy than conventional means by adjusting the propagation model.

2) Ranging Accuracy using Adaptive Scheme: To validate the effect of adaptive ranging, we add a third receiver into the setting shown in Fig. 3(a) as the ranging target, and let d_3 be its distance to the transmitter. We conduct regression using the RSS samples under three (d_1, d_2) settings, which are (2 m, 5 m), (5 m, 10 m) and (2 m, 10 m). For each settings, we estimate d_3 at $2m, 5m$ and $10m$ with our adaptive scheme, and compare it with non-adaptive scheme using the propagation model defined in [16]. Table II shows the ranging errors, where the average improvements of our adaptive ranging are approximately 33.4%, 23.1% and 33.8% under conditions C1, C2 and C3, respectively. Generally, the improvement is slight at small distance but increases greatly when d_3 becomes larger.

3) Different Numbers of Samples for Regression: Here, we observe the adaptive ranging using samples from 2, 3 and 4 devices for regression, which is shown in Fig. 4. Let d_X be the physical distance between the transmitter to device X. For each set, the adaptive ranging is conducted for device X at three different distances. Specifically, we vary d_X to be 3 m, 6 m and 9 m. Table III shows the ranging errors. Comparing to the non-adaptive scheme, the improvements on ranging accuracy using our approach are approximately 31.32%, 40.36% and 46.61% when using 2, 3, and 4 samples for regression. It implies that adaptive ranging with more regression samples is able to measure the environmental conditions more precisely, and achieve higher ranging accuracy.

TABLE II
THE COMPARISON OF RANGING ACCURACY BETWEEN NON-ADAPTIVE AND ADAPTIVE SCHEMES UNDER DIFFERENT REGRESSION CONDITIONS.

Env. cond.	d_3 (m)	non-adpative	adaptive d_1= 2 m, d_2= 5 m	adaptive d_1= 5 m, d_2= 10 m	adaptive d_1= 2 m, d_2= 10 m	improvement
C1	2	1.52 m	0.27 m	1.36 m	1.50 m	31.36%
	5	2.86 m	1.58 m	1.44 m	3.04 m	29.37%
	10	5.45 m	2.28 m	4.10 m	3.53 m	39.39%
C2	2	1.01 m	0.88 m	1.08 m	0.76 m	0.33%
	5	3.15 m	0.91 m	2.79 m	3.04 m	28.68%
	10	6.92 m	4.10 m	4.86 m	5.47 m	30.49%
C3	2	0.94 m	0.74 m	1.26 m	0.71 m	3.90%
	5	3.43 m	1.74 m	2.37 m	1.26 m	47.81%
	10	7.05 m	6.09 m	2.28 m	2.25 m	49.79%

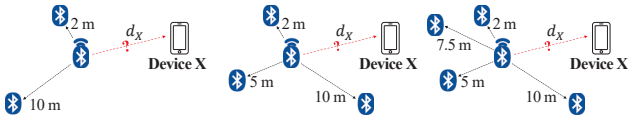

(a) 2 beacons. (b) 3 beacons. (c) 4 beacons.

Fig. 4. Experiments of adaptive ranging with different numbers of beacons.

TABLE III
ERROR OF ADAPTIVE RANGING WITH DIFFERENT NUMBER OF SAMPLES.

d_x	non-adaptive	2-sample regression	3-sample regression	4-sample regression
3 m	1.10 m	0.85 m	0.51 m	0.51 m
6 m	1.55 m	0.85 m	0.88 m	0.72 m
9 m	4.02 m	3.00 m	3.05 m	2.72 m

C. Applications of Adaptive Ranging

In order to realize adaptive ranging, we allow the BLE beacons to monitor the advertisements from others to predict the transient signal behaviours. Below, we propose two applications used in this work based on adaptive ranging concept.

1) Multi-lateration: This ranging measures the device-to-beacon (D2B) distances. An example scenario is shown in Fig. 5(a), where b_i has three neighbouring beacons b_2, b_3 and b_4. They measure the RSS of b_i's advertisements, and report to server to calculate b_i's device-specific parameters (α_i, β_i). For example, when b_2 receives b_i's advertisement, it reports the RSS P_{2i} to the server. If the server receives reports from more than two beacons, it performs regression for b_i's propagation model periodically (*e.g.* 300 s). For neighbour-less beacons such as b_k, the system uses global parameters $(\hat{\alpha}, \hat{\beta})$ regressed from all recent inter-beacon measurements to calculate the distance d_{Xk}. All signal propagation parameters are sent from server to the programmable beacons, let them embed these information in their advertisements, and send to the clients.

2) Mobile Encountering: When two devices meet up, they can receive each other's advertisements and conduct D2D adaptive ranging. A scenario is shown in Fig. 5(b). When device X measures an RSS P_{XY} from device Y, it estimates its distance d_{XY} to device Y using the propagation model with global parameters $(\hat{\alpha}, \hat{\beta})$. This D2D distance serves as indicators to calibrate the locations via updating the particle weight and distribution during PF operations.

IV. LOCALIZATION WITH ADAPTIVE RANGING

We develop a collaborative localization solution that employs inertial sensing, adaptive ranging, and mobile encountering in an environment based on BLE infrastructure. All

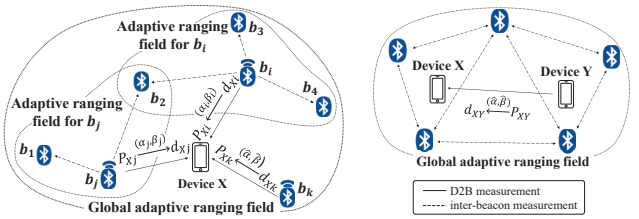

(a) Multi-lateration (b) Mobile encountering

Fig. 5. Applications of adaptive ranging.

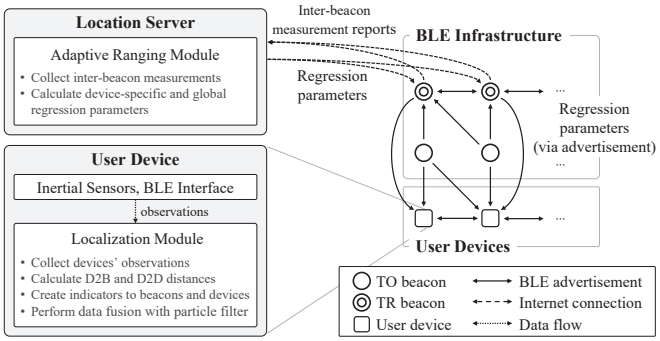

Fig. 6. The architecture of our adaptive localization system.

BLE devices are set with the same UUID in our system. The major codes determines whether the advertisement comes from a beacon or a user device, and the minor codes represents the sequential device ID in its category.

A. BLE Infrastructure and System Architecture

Fig. 6 shows our system architecture. The infrastructure contains two types of beacons: *1*) the Bluetooth 4.0 transmission-only (TO, major code `0x0014`) type, which simply advertises periodically; and *2*) the Bluetooth 4.1 transceiver (TR, major code `0x000A`), which can broadcast and receive advertisement simultaneously. TO beacons can be found easily. However, it is difficult to find TR beacons in the markets. Therefore, we program the HTC Nexus 9 tablets as our TR beacons, which advertise at 2 Hz, and report the RSS of received advertisements to the localization server at 0.1 Hz. Each report is a set of 4-element tuples representing a received advertisement, which contains: *a*) reporting time, *b*) RSS of the received advertisement, *c*) major code, and *d*) minor code, which is used as identifiers in our system.

A user device is a smartphone with inertial sensors and Bluetooth 4.1 interfaces. The inertial sensors detect human motions using the step-and-heading motion model. The Bluetooth interface broadcasts the device's location information periodically and scans for advertisements from nearby beacons. A user device can exchange location information when encountering with other devices.

In our design, the localization is performed on the client devices, while the adaptive ranging module is on the server. After regression, the server sends the device-specific and global parameter sets to all TR beacons, and the TR beacons push these parameters to the clients in its advertisements. For each TR beacon, it has to broadcast three types of

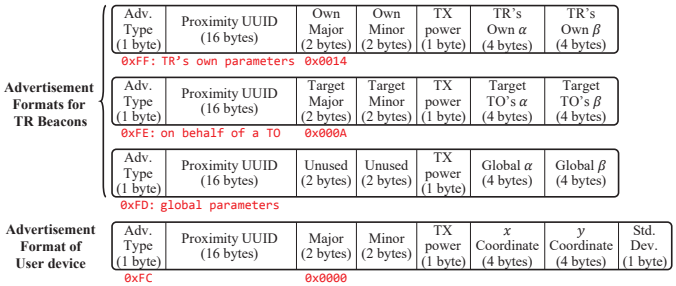

Fig. 7. The advertisement formats for TR beacons and user devices.

advertisements: *a*) with TR's own device-specific parameters, *b*) with a neighbouring TO's device-specific parameters, and *c*) with the global parameters. Due to the size limitation of the advertisement format, each advertisement can only embed one set of α and β as two 4-byte floats. Therefore, a TR beacon broadcasts it's own, all neighbouring TO's, and the global parameters in round-robin manner. The advertisement formats are shown in Fig. 7. The system uses the *advertisement type* to distinguish the packets from TR beacons and user devices. When a TR beacon advertises its own device-specific parameters, it sets the advertisement type to `0xFF`, and fills its own major, minor codes and parameters in corresponding field. When a TR advertises the parameters on behalf of a neighbouring TO beacon, it sets the advertisement type to `0xFE`, and fills the target TO beacon's major, minor code and parameters. When a TR beacon broadcasts the global parameters, it sets the advertisement type to `0xFD`, and fills the global parameters. In this way, the server and beacons form an integrated BLE-based infrastructure. On any ranging opportunities, a device first checks whether the beacon has device-specific parameters for ranging. If no, it uses the global parameters. If the global parameters are still unavailable, it uses the default propagation model in [16].

Furthermore, when an encountering event occurs among clients, the clients exchange their localization information using the BLE advertisements. Again, we modify the advertisement format to attach the information containing its estimated location (weighting centre of the particles) and the certainty of its location (standard deviation of particle set). The format is also shown in Fig. 7, where the advertisement type is `0xFC`. Note that we ignore the advertisement with location deviation larger than $10m$, which means that the certainty on that device location is low.

B. Localization Modules

Our localization system contains four primary modules: *1*) *motion detection module*, *2*) *BLE multi-lateration module*, *3*) *encounter module*, and the *4*) *particle filter*. Fig. 8 shows their organization. We address the details below:

1) Motion Detection Module: This module detects human steps and converts them into displacements. Each displacement is represented as $\vec{d_i} = s_i \cdot [\cos\theta_i, \sin\theta_i]$, where s_i and θ_i represents the step length and heading of step i. Whenever an acceleration drop over 2 ms^{-2} is detected within 0.16 s, a step event is reported. To avoid false detection, the acceleration

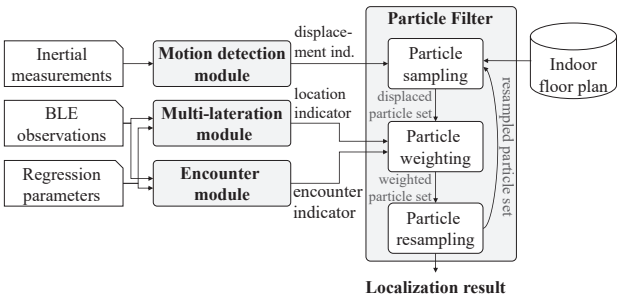

Fig. 8. The organization of the localization modules.

changes in 0.3 s after a step event are ignored. We assume that the step length s_i remains constant when walking in normal speed, and set $s_i = 0.56$ m for female and 0.65 m for male adults. On the other hand, the heading θ_i can be measured using the gyro-compass fusion technique described in [17].

2) Multi-lateration Module: This module measures nearby beacons to infer the device location. First, the device use BLE proximity detection to check whether it is in the *near* proximity of a beacon ($\simeq$3 m). If so, the device limits its possible locations within 3 m around the beacon. Otherwise, the device performs multi-lateration using the adaptively estimated D2B distances. For example, if device X obtains a BLE scan result $\{P_{Xi}|i \in \mathfrak{B}\}$, where P_{Xi} denotes the detected RSS from b_i, and $\mathfrak{B}$ is the set of detected beacons. Then, X estimates the distance $\{d_{Xi}|i \in \mathfrak{B}\}$ to each detected beacon. Since the locations of beacons are known priorly, the obtained distances can be used to infer the location ℓ_L^X of device X by applying the multi-lateration method in [18].

3) Encounter Module: This module detects encountering events between devices by measuring the BLE signals. It generates encounter indicators containing the estimated location, certainty and distance to the encountered target. An encounter event is reported if a device detects another device within a encounter range $R_e \simeq 6$ m. Specifically, if device X detects Y's advertisement, X obtains the RSS P_{XY}. It then uses the global parameters to estimate the distance d_{XY} to Y. If $d_{XY} < R_e$, then we consider that device X and Y have encountered. The encounter module on X then reports an encounter indicator with Y's estimated location ℓ_{PF}^Y, standard deviation of Y's location σ_{PF}^Y, and d_{XY} if $\sigma_{PF}^Y < 10$ m.

4) Particle Filter: A particle filter samples the distribution of possible locations as a set of particles. It tracks subjects by shifting and weighting these samples in a floorplan. The filtering process iterates through *a*) *Particle Sampling*, *b*) *Particle Weighting*, and *c*) *Particle Resampling* stages repeatedly whenever the motion detection reports a displacement. During the first iteration, we distribute the particles uniformly in the floorplan. Let $P^X(t)=\{p_j^X(t)|j \in [1, N_p]\}$ be the particle set of user X at time t, where N_p is the number of particles. Each particle $p_j^X(t)$ has two key properties:

- $p_j^X(t).loc$: the location of the particle, and
- $p_j^X(t).wt$: the weight (credibility) of the particle.

We address the details of each filtering stage below:

Particle Sampling: In this stage, we take the set $P^X(t_{i-1})$ from previous iteration as input, and shift all particles by the detected displacement $\vec{d}_i^X$, *i.e.* $p_j^X(t_i).loc = p_j^X(t_{i-1}).loc + \vec{d}_i^X + \vec{\varepsilon}_i, \forall j \in [1, N_p]$, where $\vec{\varepsilon}_i = \mathcal{N}^2(0, \sigma_{\text{IMU}}^2)$ and σ_{IMU} is the noise level of the inertial measurement units.

After moving the particles, we check whether the movement is reasonable. If the segment $\overline{p_j^X(t_i).loc, p_j^X(t_{i-1}).loc}$ intersects any walls in the floorplan, we define the movement unreasonable and set weight of these particles to zero.

Particle Weighting: In this stage, we update the weight of each particle according to the observations from multi-lateration and encounter module. Here, we define $W_L^X(\cdot)$ and $W_E^X(\cdot)$ as the weighting factors based on the multi-lateration results and encounter events. The final weight of a particle is assigned as: $p_j^X(t_i) = p_j^X(t_i).wt \times W_L^X(\cdot) \times W_E^X(\cdot)$. But in reality, these observations may not always be available. In such occasions, we set $W_L^X(\cdot) = 1$ or $W_E^X(\cdot) = 1$, accordingly.

To determine the factor $W_L^X(\cdot)$, we first check whether the multi-lateration module has reported that the device lied nearly ($\leq 3m$) to a beacon. If so, we set the weight of particles outside the region as zero. But if the weights of all particles are set to zero, we shift all particles to the location of that beacon and restart from the sampling stage. If no beacon is nearby, we refer the location from multi-lateration ℓ_L^X and derive the weighting factor of multi-lateration for all particles $j \in [1, N_p]$:

$$W_L^X(\ell_L^X, j, t_i) = \exp\left(-\frac{\|p_j^X(t_i).loc - \ell_L^X\|^2}{2\sigma_L^2}\right), \tag{3}$$

where σ_L^2 is the error tolerance of multi-lateration procedure.

To determine the factor $W_E^X(\cdot)$ for device X, we first derive an individual weighting factor $W_E^{XY}(\cdot)$ derived from an encounter event with Y, which is formulated as:

$$W_E^{XY}(\ell_{PF}^Y, \sigma_{PF}^Y, j, t_i) = \exp\left(-\frac{(\|\overline{p_j^X(t_i).loc, \ell_{PF}^Y}\| - d_{XY})^2}{2(\sigma_{PF}^Y + \sigma_E)^2}\right), \tag{4}$$

where ℓ_{PF}^Y is the estimated location of Y, σ_{PF}^Y is the standard deviation of Y's particles (embedded in Y's advertisements), d_{XY} is the estimated D2D distance to Y, and σ_E is the noise level of the distance measurement. As multiple encounter events may occur simultaneously, the overall weighting $W_E^X(\cdot)$ of encountering for all particles $j \in [1, N_p]$ is defined as:

$$W_E^X(\mathfrak{E}, j, t_i) = \prod_{Y \in \mathfrak{E}} W_E^{XY}(\ell_{PF}^Y, \sigma_{PF}^Y, j, t_i), \tag{5}$$

where $\mathfrak{E}$ is the set of devices that X has encountered.

Particle Resampling: In this final filtering stage, we compute and report the weighted centre ℓ_{PF}^X of the particle set $P^X(t)$ as the localization result of device X, which is defined as:

$$\ell_{PF}^X = \frac{\sum_{j=1}^{N_p} p_j^X(t_i).loc \times p_j^X(t_i).wt}{\sum_{j=1}^{N_p} p_j^X(t_i).wt}. \tag{6}$$

After reporting the user's location, we form a new particle set by randomly selecting a particle in the current set $P^X(t_i)$ and add it to the new set $P^X(t_{i+1})$ for N_p times. The probability of particle $p_j^X(t_i)$ being picked is

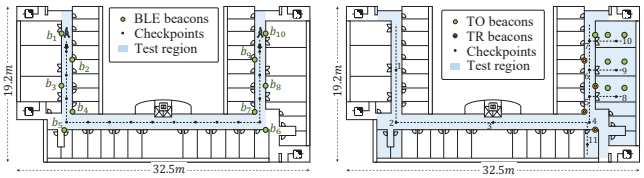

(a) (b)

Fig. 9. The environment configurations for the (a) corridor experiment, and (b) rooms with corridor experiment.

$p_j^X(t_i).wt / \sum_{k=1}^{N_p} p_k^X(t_i).wt$. After a particle is picked, we keep the location of the selected particle $p_j^X(t_{i+1}).loc = p_j^X(t_i).loc$, but assign a uniform weight N_p^{-1}. Finally, the resampled particle set is passed to the next iteration.

V. Field Experiments

In this section, two sets of experiments are presented: *a*) the corridor experiment, where we focus on observing individual effects; and *b*) the rooms with corridor experiment, where we can observe the performance in a realistic indoor environment.

A. Corridor Experiment

To verify the performance of the proposed localization system, two subjects X and Y are told to walk in a U-shape corridor and encounter with each other in the middle. We examine and compare the performances of three different localization methods: *a*) localization with non-adaptive ranging, *b*) localization with adaptive ranging using global parameters, and *c*) localization with adaptive ranging using device-specific parameters if possible. The environment is shown in Fig. 9(a), but with different beacon configurations. For method *a*), we deploy 10 TO beacons along the corridor, which are labelled as $b_1, b_2, ..., b_{10}$. For methods *b*) and *c*), we replace beacons b_2, b_4, b_7 and b_9 with TR beacons to collect inter-beacon measurements for adaptive ranging. The regressions are performed every 600 s.

The average error distances of methods *a*), *b*) and *c*) are approximately 1.88 m, 1.55 m and 1.35 m. About 80% of the errors lie within 3.02 m, 2.41 m, and 2.13 m; while the maximum error distances are approximately 4.36 m, 3.91 m, and 3.86 m when applying method *a*), *b*), and *c*), respectively.

To further observe the details, we plot the localization results and the standard deviations of particles for each experiment sets, as shown in Fig. 10. First, we observe the effect of adaptive ranging. One can observe that subject X's errors before the encountering events are approximately 3.42 m, 1.73 m and 1.49 m when using *a*), *b*) and *c*), respectively; while Y's errors are 4.26 m, 1.29 m and 1.10 m, under the same cases. We can conclude that adaptive ranging using device-specific parameters is more accurate than using the global ones, and they both outperform the non-adaptive method.

Second, we discuss the effect of signal obstructions. One can observe that the estimated locations deviate from the actual paths when subjects enter the corner regions. For subject X, we extract three periods around the left corner, which are: i) 10 steps before entering the corner region, ii) when the subject turns around the corner (orientation changes $\geq 10°$), and iii) 10 steps after turning and before M2M encountering. Similarly, the same periods are extracted from Y's results around the right corner. The errors are shown in Table IV.

TABLE IV
The localization error near the corner regions.

	X's localization error			Y's localization error		
period	*a*)	*b*)	*c*)	*a*)	*b*)	*c*)
i)	3.26 m	2.47 m	2.21 m	2.48 m	1.96 m	1.94 m
ii)	4.08 m	3.81 m	3.94 m	3.21 m	2.88 m	2.74 m
iii)	3.84 m	3.23 m	2.63 m	2.84 m	2.06 m	2.10 m

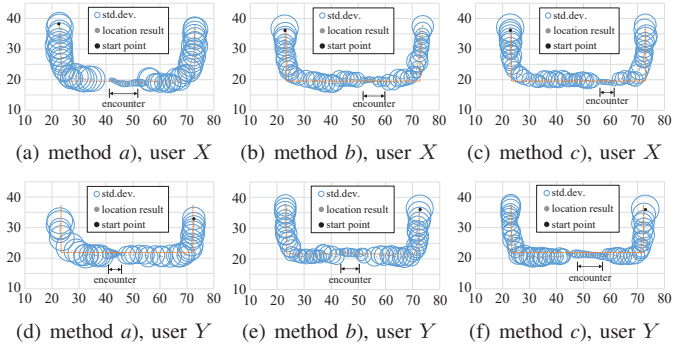

(a) method *a*), user X (b) method *b*), user X (c) method *c*), user X

(d) method *a*), user Y (e) method *b*), user Y (f) method *c*), user Y

Fig. 10. Localization results of both subjects in the corridor experiment.

Third, we observe the effect of encountering. We can observe from Fig. 10 after X and Y encountered, both their localization error and the deviation are decreased. For subject X, the localization errors drop from 3.42 m to 0.67 m in method *a*), from 1.22 m to 0.63 m in *b*), and from 1.10 m to 0.64 m in method *c*); while Y's errors drop from 1.71 m to 0.61 m, from 1.12 m to 0.56 m, and from 1.10 m to $0.43m$ in methods *a*), *b*) and *c*), respectively. The standard deviations of X's particles are decreased by 4.02 m, 1.45 m and 1.38 m; and Y's deviations are decreased by 2.57 m, 0.91 m and 1.81 m in methods *a*), *b*) and *c*), respectively.

B. Rooms with Corridor Experiment

In this experiment, we wish to observe how common indoor structures affect the localization results. We deploy 4 TR beacons and 7 TO beacons on the right side of the floorplan, and allow the subjects to move into some rooms. The results are shown in Fig. 11. Here, we pick 11 checkpoints and compare the localization results under two configurations: *a*) localization with non-adaptive ranging, and *b*) localization

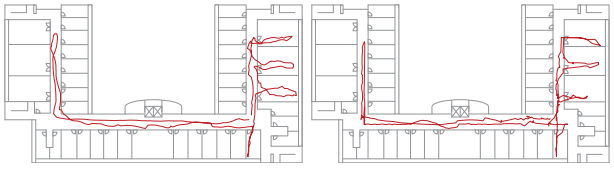

(a) method *a*), user X (b) method *a*), user Y

Fig. 11. The estimated user trajectories in the rooms with corridor experiment.

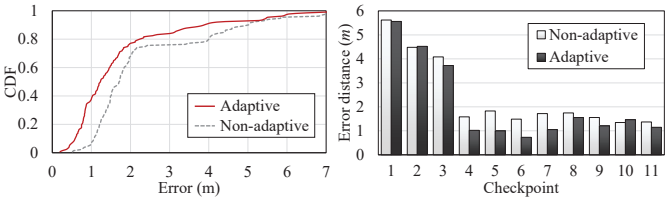

(a) CDF of localization error. (b) Error on each checkpoint.

Fig. 12. The localization results of the rooms with corridor experiment.

with adaptive ranging using device-specific parameters if possible. The environment configuration is shown in Fig. 9(b).

Among the 11 checkpoints, checkpoints 1-3 are not covered by BLE infrastructure. Checkpoints 4-7 lie in the corridor within infrastructural coverage. Checkpoints 8-10 lie inside the rooms, which are covered by TO beacons, while checkpoint 11 lies in a room without any TO beacons. Fig. 12(a) shows the CDF of localization error, and Fig. 12(b) shows the error on each checkpoint. One can observe that our adaptive localization scheme outperforms the conventional means.

We can further investigate the details by separating the checkpoints according to their locations. On checkpoints 1-3, the improvement is only 2.98%, which is quite negligible. This is because that only checkpoint 3 is on the fringe of beacon coverage, while checkpoints 1 and 2 do not have such benefit. On checkpoints 4-7, where the line-of-sight measurements dominates the BLE ranging procedures, the improvements are significant, which is approximately 42.67%. On checkpoints 8-11, the improvements on accuracy is only 9.89%. This is because that TR beacons are obstructed and cannot estimate the correct propagation models, causing the adaptive ranging modules to create an inaccurate model and therefore lower the ranging accuracy. This effect can be observed on checkpoint 10, where there is a wall between the TO and TR beacons. However, if the floorplan is a prior knowledge to the system, we can filter out these obstructed samples for regression, and derive more accurate relations.

VI. Conclusions

In this research, we propose to improve the BLE wireless positioning with adaptive ranging, to reduce the localization error cause by device and environmental conditions. It uses the inter-beacon measurements to measure the transient conditions and adjust the parameters of signal propagation models used to convert the RSS into distance estimations. These benefits are validated in Section III. To realize the concept, we design a particle-filter-based localization model that fuses the inertial data, adaptive multi-lateration results and mobile encountering together to locate a target. Finally, we perform two sets of field experiments in a department building. In the corridor experiment, where most of the measurements are acquired in line-of-sight, the improvements on localization accuracy are significant. Comparing to the non-adaptive scheme, the accuracy improvements are approximately 17.56% and 28.19% when using adaptive ranging with global and device-specific parameters, respectively. In the rooms with corridor experiment, our system which utilizing the adaptive ranging with device-specific parameters has an improvement of approximately 19.99% in accuracy. Our experiments have shown that with the adaptive ranging techniques, the localization system gains the capabilities to "sense" the environment and calibrate itself, therefore, generating more accurate results.

References

[1] P. Bahl and V. N. Padmanabhan, "RADAR: An in-building RF-based user location and tracking system," in *IEEE Infocom*, vol. 2, 2000, pp. 775–784.

[2] D. Niculescu and B. Nath, "Ad-Hoc positioning system (APS) using AoA," in *IEEE Infocom*, vol. 3, 2003, pp. 1734–1743.

[3] A. Savvides, C.-C. Han, and M. B. Strivastava, "Dynamic fine-grained localization in Ad-Hoc networks of sensors," in *ACM/IEEE Mobicom*, 2001, pp. 166–179.

[4] H. K. Fard, Y. Chen, and K. K. Son, "Indoor positioning of mobile devices with agile ibeacon deployment," in *IEEE Canadian Conf. Elect. and Comput. Eng.* IEEE, 2015, pp. 275–279.

[5] A. Thaljaoui, T. Val, N. Nasri, and D. Brulin, "BLE localization using RSSI measurements and iRingLA," in *IEEE Int. Conf. Ind. Tech.* IEEE, 2015, pp. 2178–2183.

[6] D. Schwarz, M. Schwarz, J. Stückler, and S. Behnke, "Cosero, find my keys! object localization and retrieval using bluetooth low energy tags," in *Proc. RoboCup Int. Symp.*, 2014.

[7] P. Krishnan, A. Krishnakumar, W.-H. Ju, C. Mallows, and S. Gamt, "A system for lease: Location estimation assisted by stationary emitters for indoor rf wireless networks," in *Proc. of IEEE INFOCOM*, vol. 2. IEEE, 2004, pp. 1001–1011.

[8] J. Yin, Q. Yang, and L. M. Ni, "Learning adaptive temporal radio maps for signal-strength-based location estimation," *IEEE Trans. on Mobile Comput.*, vol. 7, no. 7, pp. 869–883, 2008.

[9] Y.-C. Chen, J.-R. Chiang, H.-h. Chu, P. Huang, and A. W. Tsui, "Sensor-assisted wi-fi indoor location system for adapting to environmental dynamics," in *Proc. ACM Int. Symp. on Modeling, anal. and simulation of wireless and mobile syst.* ACM, 2005, pp. 118–125.

[10] C.-C. Lo, L.-Y. Hsu, and Y.-C. Tseng, "Adaptive radio maps for pattern-matching localization via inter-beacon co-calibration," *Pervasive and Mobile Comput.*, vol. 8, no. 2, pp. 282–291, 2012.

[11] F. Li, C. Zhao, G. Ding, J. Gong, C. Liu, and F. Zhao, "A reliable and accurate indoor localization method using phone inertial sensors," in *Proc. ACM Conf. on Ubiquitous Comput*, 2012, pp. 421–430.

[12] M. Alzantot and M. Youssef, "UPTIME: Ubiquitous pedestrian tracking using mobile phones," in *IEEE Wireless Commun. and Networking*, 2012, pp. 3204–3209.

[13] A. Doucet, S. Godsill, and C. Andrieu, "On sequential Monte Carlo sampling methods for Bayesian filtering," *Stat. and Comput.*, vol. 10, no. 3, pp. 197–208, 2000.

[14] H. Liu, Y. Gan, J. Yang, S. Sidhom, Y. Wang, Y. Chen, and F. Ye, "Push the limit of WiFi based localization for smartphones," in *ACM Mobicom*, 2012, pp. 305–316.

[15] J. Jun, Y. Gu, L. Cheng, B. Lu, J. Sun, T. Zhu, and J. Niu, "Social-Loc: Improving indoor localization with social sensing," in *Proc. ACM Conf. Embedded Networked Sensor Syst.*, 2013, pp. 1–14.

[16] "The open and interoperable proximity beacon specification," Altbeacon, 2015.

[17] P. Lawitzki and J. Charzinski, "Application of dynamic binaural signals in acoustic games," Dec. 2011.

[18] W. Murphy and W. Hereman, "Determination of a position in three dimensions using trilateration and approximate distances," 1995.